Kinetics of Water Absorption and Hygrothermal Aging Rubber Toughened Poly(Butylene Terephthalate) With and Without Short Glass Fiber Reinforcement

B. N. Yow,[1] U. S. Ishiaku,[1] Z. A. Mohd Ishak,[1] J. Karger-Kocsis[2]

[1]*School of Materials & Mineral Resources Engineering, Universiti Sains Malaysia, 14300 Nibong Tebal Penang, Malaysia*
[2]*Institute For Composite Materials Ltd., University of Kaiserslautern, P.O. Box 3049, D-67663 Kaiserslautern, Germany*

Received 10 February 2003; accepted 14 October 2003

ABSTRACT: The objectives of this paper were to investigate the water absorption and hygrothermal aging behavior of rubber-toughened poly(butylenes terephthalate) (RT-PBT) with and without short glass fiber (SGF) reinforcement. The rubbers used in the study were AX8900 and EXL2314, both of which are acrylate-based terpolymer. The effect of the hygrothermal aging on its fracture properties was also studied. The kinetics of the water absorption study were carried out on the injection-molded samples of the RT-PBTs and the SGF-reinforced rubber-toughened PBT (SGF-RT-PBT) at three immersion temperatures, 30, 60 and 90°C, for a total of 450 h. The study of the deterioration caused by the hygrothermal aging was conducted by investigating the fracture parameters and flexural properties of all the materials as both hygrothermally aged (HA) and redried state (RD). The modes of the failure of HA and RD samples were studied using the scanning electron microscopy (SEM) technique. It was found that all the samples conformed to Fickian behavior and the kinetics of absorption exhibited a strong dependency on the rubber types, presence of SGF, as well as the immersion temperature. Generally, SGF-RT-PBT showed a better resistance to hygrothermal aging than that of RT-PBT and PBT, though a declining trend was observed in the fracture parameters, K_c and G_c. However, an opposite observation was exhibited in the flexural properties in some, but not all cases. Finally, the results obtained from SEM micrographs showed that permanent damage occurred in the materials and the hygrothermal aging had suppressed the plastic deformation ability of the PBT matrix and both types of impact modifiers where brittle failure was observed. Fiber pull-out was apparently the failure mode of the SGF-reinforced materials. J Appl Polym Sci 92: 506–516, 2004

Key words: poly(butylene terephthalate); rubber toughened; short glass fiber reinforced; water absorption; hygrothermal aging; fracture toughness; flexural properties

INTRODUCTION

Poly(butylene terephthalate) (PBT) is a semicrystalline engineering thermoplastic that is mostly used in the electrical appliance, automobile, and army appliance industries. The good thermal, chemical, physical, electrical, and mechanical properties have enabled PBT to be the choice when it comes to material selection to meet high service requirements. Generally good processing characterization via short extrusion and injection molding cycles and excellent mold flow are additional advantages of PBT. However, PBT has two major drawbacks that have limited its usage: (i) it shows a strong tendency for brittle fracture when subjected to high-speed testing and (ii) it undergoes hydrolysis that leads to serious embrittlement when subjected to hygrothermal aging (HA) especially at high temperatures and in moist environments.

Approaches recognized to overcome the first drawback of PBT are production of a completely new polymer based upon a novel monomer[1] or modification of the existing polymers through incorporation of short glass fiber, block copolymer, structural foams, and rubber.[1] Part I of this investigation reported the effect of rubber inclusion on the fracture properties of PBT.[2]

PBT, being a polyester, is susceptible to hydrolysis when exposed to high temperature and moist environment. The hydrolysis behavior of neat PBT is well documented.[3] However, toughening of PBT by the inclusion of various types of rubbers and their effect on its hygrothermal aging behavior is of special interest. So far, studies of the hygrothermal aging have focused on PBT/PC blend.[4] Publications on hygrothermal aging study of rubber-toughened (RT)-PBT are rather limited. A recent hygrothermal aging study on styrene-acrylonitrile/acrylate-based core shell rub-

Correspondence to: Z. A. M. Ishak (zarifin@eng.usm.my).

ber- toughened PBT (CSR-PBT) was carried out by Mohd Ishak et al.[5,6] The results obtained showed that the CSR with a rigid shell failed to improve the toughness of PBT. The CSR-PBT also showed poor resistance to hygrothermal aging at 90°C.

Experimental

Materials and processing

Materials

The PBT used was a flame retardant injection molding grade (Valox 310 SEO, GE Plastics). The specific gravity is 1.39 g/cm^3 and melt flow index is 7 g/10 min (Load = 2.16 kg, 250°C). AX8900 is ethylene-*co*-glydicyl methacrylate-*co*-methacrylate terpolymer (E/GMA/MA), which comprises 21–26 wt % acrylate and 6.5–8 wt % GMA. The melting point of AX8900 is 65°C and the glass transition temperature is −40°C. Its melt flow index is 6 g/10 min. EXL2314 comprises alkyl acrylate, alkyl methacrylate, and glycidyl methacrylate terpolymer, which is an all-acrylic product. The melting point and glass transition temperatures are 120 and –15°C, respectively. 10 wt % of both acrylate rubbers was incorporated into PBT matrix and considered as the RT-PBT material in this study while RT-PBT containing 30 wt % short glass fiber (SGF; Maxi-Chop 3790) are designated as SGF-RT-PBT. The diameter and cut length of the glass fiber were 13 μm and 4 mm, respectively. It has a density of 2.65 g/cm^3 and was treated with silane.

Processing

RT-PBT and SGF-RT-PBT were compounded using a HAAKE model counter-rotating twin screw extruder Rheomex CTW 100 using a speed of 22 rpm and temperature profile 150–240°C from feeding zone to the die zone. The extrudate was pelletized with a HAAKE pelletizer. Film-gated rectangular plaques of dimension 149 × 149 × 3 mm^3 were injection molded from the pellets on a Battenfled Unilog 350CD injection molding machine. Melt and mold temperatures of 265 and 60°C, respectively, were used.

Kinetics of moisture absorption

All specimens were vacuum dried at 100°C for 4 h and the dry weight, W_d, of the specimens was recorded. They were then immersed in distilled water at 30, 60, and 90°C. Weights of the specimens immersed in the water were recorded periodically on a Sartorius BP221S weighing balance with a precision of 0.1 mg.

The percentage weight gain at any time, M_t, as a result of water absorption was determined by:

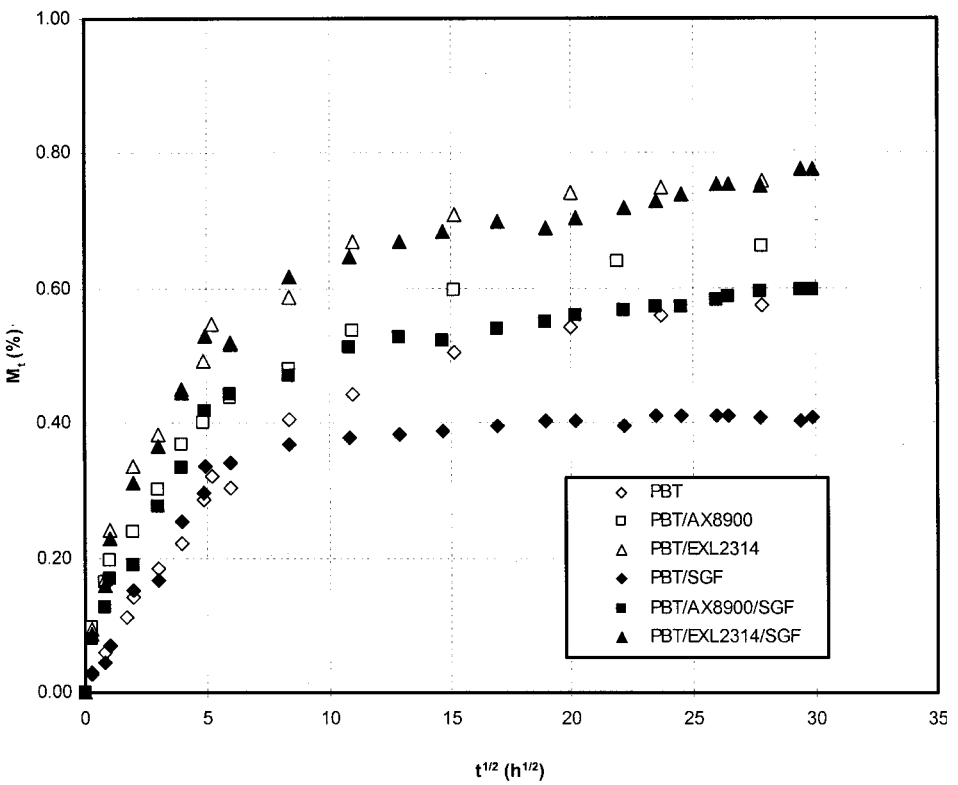

Figure 1 Water absorption curve of various grades of PBT materials at immersion temperature of 90°C.

TABLE I
***D* and M_m Values of All Materials Immersed in 30, 60, and 90°C Distilled Water**

	30°C		60°C		90°C	
	M_m (%)	$D \times 10^{-7}$ (m^2/h)	M_m (%)	$D \times 10^{-7}$ (m^2/h)	M_m (%)	$D \times 10^{-7}$ (m^2/h)
PBT	0.20	4.65	0.32	16.91	0.58	44.08
PBT/AX8900	0.24	7.59	0.38	26.81	0.66	54.59
PBT/EXL2314	0.28	14.09	0.46	32.62	0.76	101.59
PBT/SGF	0.19	2.76	0.37	13.63	0.41	40.43
PBT/AX8900/SGF	0.26	3.10	0.40	17.55	0.60	44.07
PBT/EXL2314/SGF	0.28	3.47	0.51	19.91	0.78	45.57

$$M_t(\%) = (W_w - W_d)/W_d \times 100 \quad (1)$$

where W_w denotes the weight of the wet material. The equilibrium moisture absorption or maximum moisture content, M_m, was calculated as an average value of several consecutive measurements at the maximum values obtained after an exposure period of 450 h.

The weight gain resulting from moisture absorption can be expressed in terms of two parameters, the diffusion coefficient or diffusivity, D, and M_m, as:[4]

$$M_t = M_m\left\{1 - \frac{8}{\pi^2}\exp\left[-\left(\frac{Dt}{h^2}\right)\pi^2\right]\right\} \quad (2)$$

where t is the time and h is the thickness of the specimen.

Fracture test

Compact tension (CT) specimens with a notch length, a = 20 mm; free ligament width, W = 50 mm were machined from the injection-molded plaques. Specimens with an initial notch cut transverse to the melt flow direction were designated as L-T according to the ASTM E606–81 standard as detailed in Part I.[2] Prior to the static loading tests the notch of the CT was sharpened with a fresh razor blade. Fracture toughness determinations were performed on a Tensometric testing machine. Crosshead speed of 1 mm/min was employed. The fracture toughness (K_c) and fracture energy (G_c) were calculated in accordance with the recommendation of the protocol of Linear Elastic Fracture Mechanics (LEFM) Standard.[7,8] In all cases, three CT specimens of each material were tested. A flexural test was also performed on a Testometric Testing machine in accordance to ASTM D790. Crosshead speed and span of 2 mm/min and 50 mm, respectively, were employed. Five test specimens with 12.70 × 3.00 mm (width × thickness) were tested in each case.

Conditioning of specimens

Due to the hygroscopic nature of PBT, all testing specimens were placed in a vacuum oven at 80°C for 24 h prior to testing. Upon removal from the oven, the specimens were allowed to cool to room temperature inside desiccators to maintain a standard moisture content for all specimens. These specimens are then regarded to be in the as received (AR) state. For the hygrothermal aging study, the specimens were immersed in distilled water at 30, 60, and 90°C. Once the water uptake in the specimens had reached a saturation limit, both CT and flexural tests were carried out as described under Fracture test. Further investigation into the extent of deterioration of the fracture and flexural properties of the specimens was carried out by redrying the specimens (RD) in a vacuum oven at 100°C for 24 h.

Fractography

The failure mode of the fractured CT was determined with a Leica Cambridge scanning electron microscope (SEM). SEM micrographs were taken at 10 kV acceleration voltage at various magnifications. Prior to the SEM observations the fractured parts were mounted on an aluminum stub and sputter coated with a thin layer of gold to avoid electrical charging during examination.

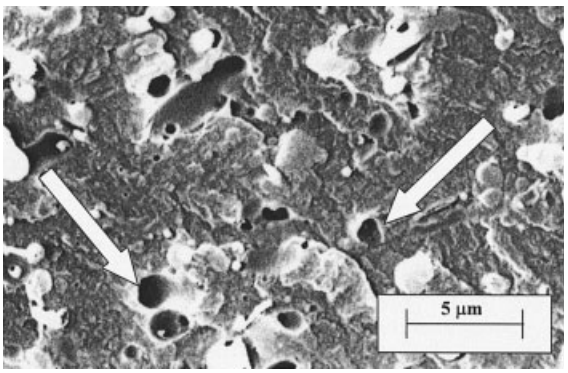

Figure 2 SEM micrograph showing the microcracks occurring on RD (90°C) PBT matrix due to moisture attack (white arrows).

TABLE II
Theoretical and Experimental Values of M_m of SGF-PBT and SGF-RT-PBT Immersed in Distilled Water at 90°C

	Experimental	Theory I	Theory II
PBT/SGF	0.407	0.406[a] (0.003)	0.447[a] (0.10)
PBT/AC8900/SGF	0.596	0.348[a] (0.42)	0.479[a] (0.20)
		0.462[b] (0.22)	0.522[b] (0.12)
PBT/EXL2314/SGF	0.776	0.348[a] (0.55)	0.421[a] (0.46)
		0.532[b] (0.30)	0.529[b] (0.32)

Values in parentheses are the deviance from the experimental values reported as percentages.
[a] PBT matrix as the continuous phase.
[b] RT-PBT matrix as the continuous phase.

RESULTS AND DISCUSSION

Kinetics of water absorption

Figure 1 shows the percentage moisture absorption, M_t, of all the materials as a function of $t^{1/2}$ at immersion temperature of 90°C. The initial linear relationship between M_t and $t^{1/2}$ was clearly observed in each material followed by the abscissa. This indicates that Fickian behavior was conformed by the RT-PBT and SGF-RT-PBT samples. Similar observations were obtained for immersion temperatures of 30 and 60°C, albeit with a slower absorption process as the temperature decreased. The diffusion coefficient, D, and maximum moisture content, M_m, are tabulated in Table I. The D and M_m values obtained indicate that the water absorption parameter was a function of immersion temperature. This can be attributed to the temperature controlled diffusion mechanism in which molecular activity is enhanced as temperature increased. Similar observations have been reported for thermoplastic

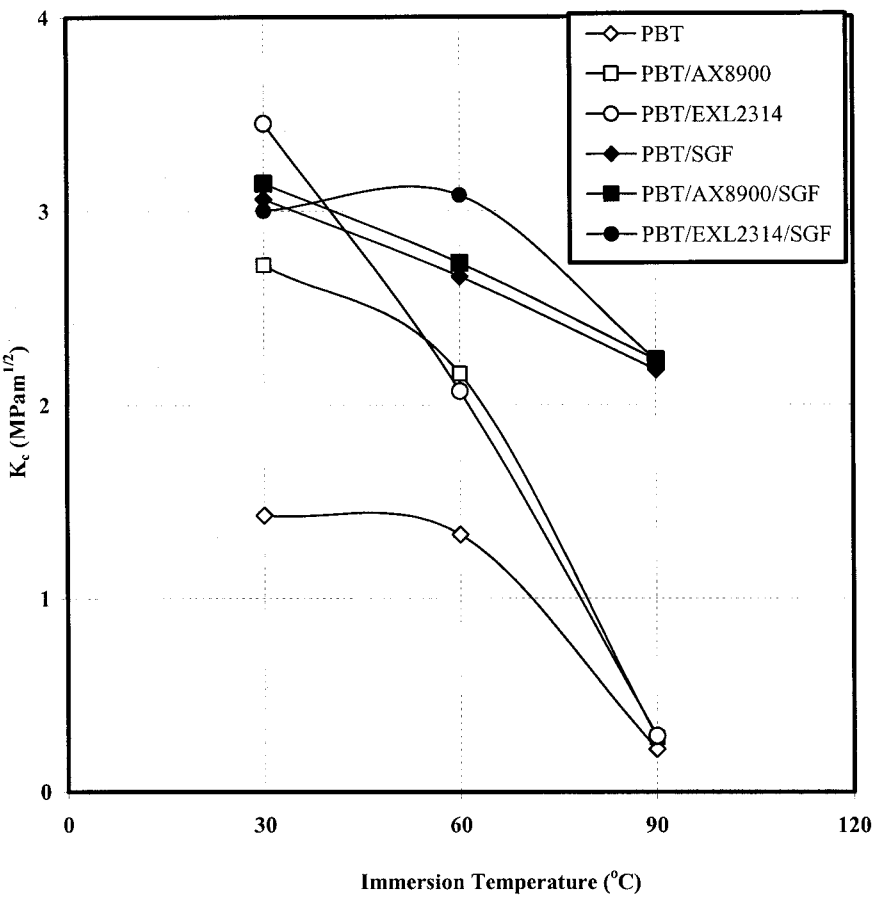

Figure 3 Effect of immersion temperature on K_c of various grades of PBT materials.

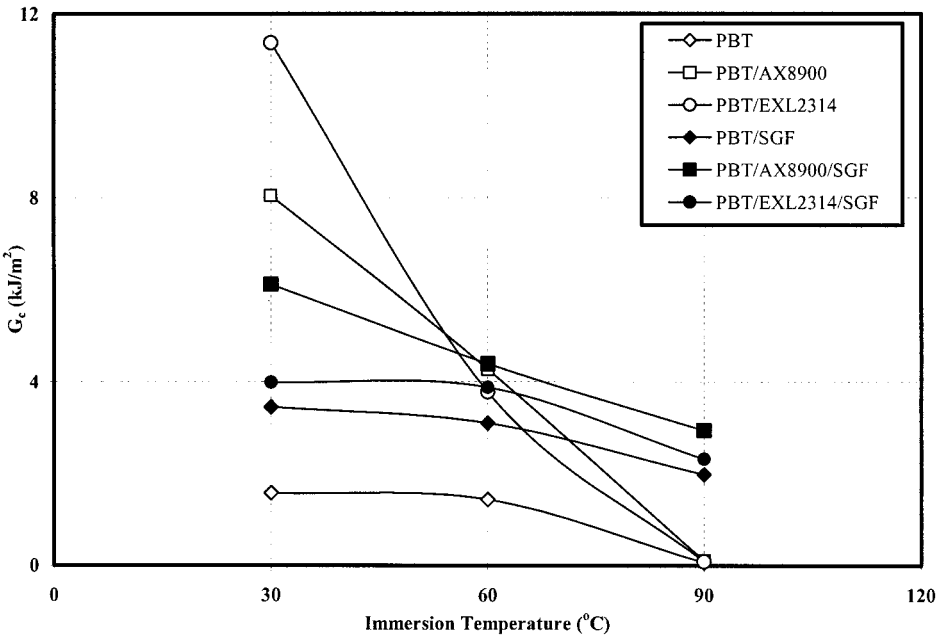

Figure 4 Effect of immersion temperature on G_c of various grades of PBT materials.

and thermoset based composites.[5,6,9–11] It was also observed that the increase of M_m and D values is more apparent when the temperature increases from 60 to 90°C. This is due to the flexibility of PBT, which increased above its T_g at ~ 65°C. The movement of the PBT chains permitted more free volume for water absorption. Besides that, the microdefects in the form of microcracks and pores caused by the attack of water molecules also contributed to the increase of D and M_m values. This is more significant at higher immersion temperatures as the hydrolysis tendency of PBT increases at high temperatures.[3] The SEM micrograph in Figure 2 shows the occurrence of microcracks due to the effect of moisture attack.

Table I also shows that the M_m and D values of PBT increased as AX8900 and EXL2314 were incorporated. This is due to the hygroscopic nature of the acrylate rubber in AX8900 and EXL2314.[12] It is also observed that materials modified by EXL2314 showed higher M_m and D values than those of AX8900. This may be attributed to the higher content of acrylate composition in EXL2314 (100%) than AX8900 (28%). However, the incorporation of nonhygroscopic SGF reinforcement[13] retarded the water absorption in the subsequent composites, i.e., PBT/SGF, PBT/AX8900/SGF, and PBT/EXL2314/SGF. The M_m and D values obtained are much lower than those without SGF reinforcement. The complex orientation of SGF in the matrix had restricted the diffusion of water molecules into the matrix. Mohd Ishak et al.[9,10] have also reported that the M_m and D values are dependent on fiber loading in PBT and PA 66 composites. Mohd Ishak and Berry[10] calculated M_m using the following relation:

$$(M_m)_c = (M_m)_r \times W_r \quad (3)$$

where $(M_m)_c$ and $(M_m)_r$ represent equilibrium moisture content of the composite and unreinforced continuous phase, respectively. W_r is the weight fraction of the continuous phase in the composite. Another theory developed by Valentin et al.[14] attributed the total moisture absorbed by the composite $(M_m)_c$ to the following relation:

$$\frac{(M_m)_c}{(M_m)_m} = \frac{\rho_m}{\rho_c}(1 - V_f) \quad (4)$$

where ρ is the density and subscript m and c are the continue phase and composite, respectively. V_f is the volume fraction of the glass fiber.

Theoretical values of $(M_m)_c$ were calculated using eqs. (3) and (4) and are tabulated in Table II. In the

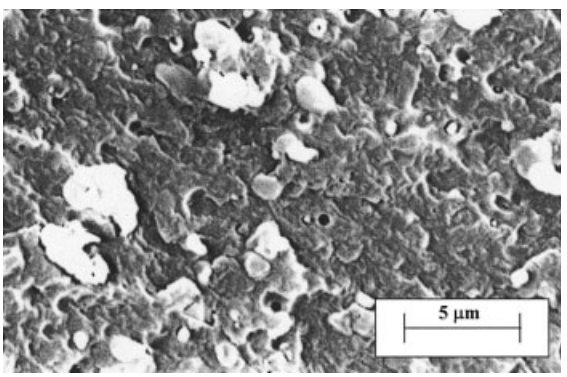

Figure 5 SEM micrograph of HA (90°C) specimen of PBT.

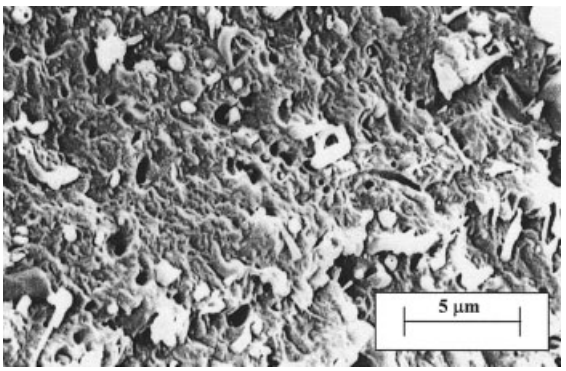

Figure 6 SEM micrograph of HA (90°C) specimen of PBT/AX8900.

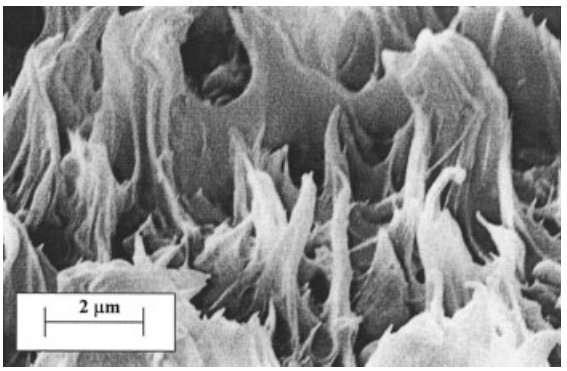

Figure 8 SEM micrograph of AR specimen of PBT.

case of the ternary system, the theoretical $(M_m)_c$ value was calculated by taking into consideration the RT-PBT matrix phase as the continuous phase in the system. The assumption that the SGF did not absorb moisture was taken into account. The results showed that the experimental values of M_m were different from theoretical values. However, eq. (4) developed by Valentin et al.[14] gave a closer result to the experiment values. This indicates that eq. (4) is more accurate in predicting the moisture content in the ternary system of SGF-RT-PBT. Results obtained for $(M_m)_c$ calculated using method (a) where PBT matrix is taken as the continuous phase and (b) where RT-PBT matrix as the continuous phase also indicated that the phase responsible for the water absorption was the rubber modified PBT matrix (see Table II). The presence of the microvoids[15] is believed to be responsible for the deviation of the experimental values from the theoretical values.

Effect of hygrothermal aging

Fracture toughness

Figures 3 and 4 show the effect of the immersion temperature on the fracture parameters, i.e., K_c and G_c, respectively, of all grades of PBT materials. In all cases, K_c and G_c dropped as the immersion temperature increased from 30 to 90°C. In the range of immersion temperatures from 30 to 60°C, the K_c value of PBT/EXL2314 deteriorated more apparently compared to those for PBT and PBT/AX8900. This indicates that PBT/EXL2314 has inferior resistance to hygrothermal aging compared to PBT/AX8900. However, K_c of PBT and RT-PBT dropped drastically when the temperature increased to 90°C. This may be attributed to the severe hydrolysis of PBT matrix. Golovoy et al.[4] reported a drastic reduction of the molecular weight of PC/PBT blend and formation of some low-molecular-weight fractions after 15 days of immersion in water at 98°C. The hydrolysis of PBT matrix was evident from SEM micrographs as indicated in Figures 5-7 for hygrothermally aged PBT, PBT/AX8900, and PBT/EXL2314 specimens, respectively, compared to its corresponding AR specimens as seen in Figure 8-10. The SEM micrographs also revealed a brittle fracture mode where there was no yielding of the PBT matrix observed. The plastic deformation in the form of matrix drawing or shear yielding that is believed to be responsible for the ductility of the matrix is totally corrupted after hygrothermal aging at 90°C; thus explaining the dramatic reduction of K_c and G_c values (Table II).

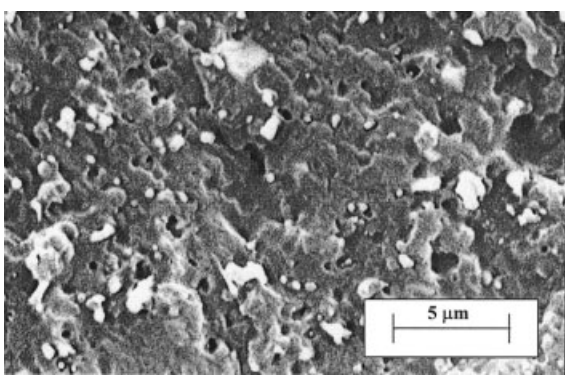

Figure 7 SEM micrograph of HA (90°C) specimen of PBT/EXL2314.

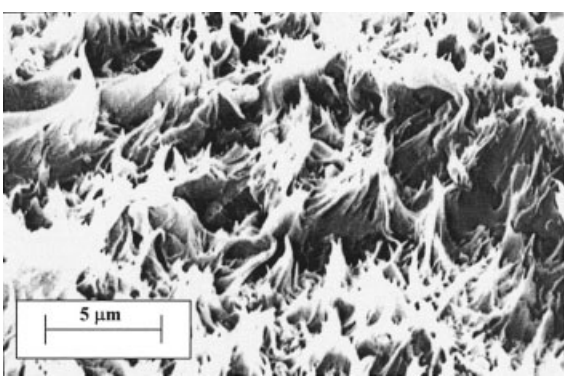

Figure 9 SEM micrograph of AR specimen of PBT/AX8900

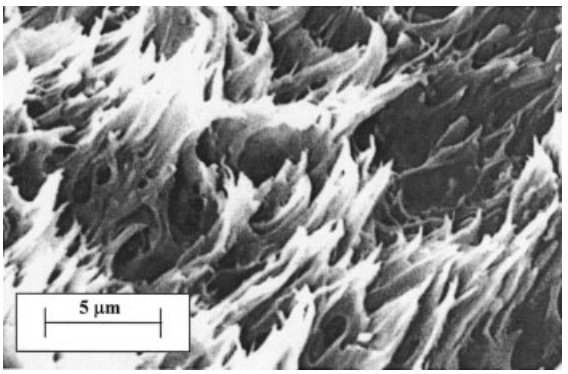

Figure 10 SEM micrograph of AR specimen of PBT/EXL2314.

From Table III, the SGF reinforced grades, i.e., PBT/SGF, PBT/AX8900/SGF, and PBT/EXL2314/SGF showed higher resistance to hygrothermal aging. K_c of various PBT composites were in the range of 2.18–2.23 $MPam^{1/2}$ while 0.22–0.29 $MPam^{1/2}$ was reported for the corresponding unreinforced grades. Similar trend was also observed for G_c. Fiber pull out was the dominant failure mode. This explained the high % retention (65%) in K_c value of PBT/SGF. The presence of SGF is also believed to have protected the PBT matrix from being hydrolyzed. The complex orientation of SGF obstructed the diffusion of absorbed water molecules into the matrix and hence reduced the extent of the hydrolysis of PBT matrix. This is evident from the SEM micrograph where yielding of PBT matrix was observed especially at the root of the fiber pulled out as seen in Figure 11 for the RD PBT/SGF specimen. For the ternary system, i.e., PBT/AX8900/SGF and PBT/EXL2314/SGF, fiber pull out can be seen in Figures 12 and 13, respectively. This also explained the similar values of K_c of all three SGF-reinforced materials, i.e., PBT/SGF, PBT/AX8900/SGF, and PBT/EXT2314/SGF, which are higher than those for non-SGF-reinforced materials, as can be seen in Figure 3.

The extent of the deterioration caused by the hygrothermal aging was investigated by redrying the specimen to remove the absorbed water molecules. The results are shown in Table III. It can be seen that, irrespective of immersion temperature, the toughness of the materials was not fully recovered upon redrying the specimens. The reinforced grades, however, showed better % recovery in the toughness than the unreinforced grades. This proved that the presence of SGF has imparted protection to the subsequent composites from the hydrolysis process. This can be evidenced also from SEM micrographs in Figures 12 and 13 for PBT/AX8900/SGF and PBT/EXL2314/SGF, respectively. A small degree of matrix yielding was observed compared to the smooth fracture surface in PBT (Figs. 2 and 5). Mohd Ishak et al. also reported a similar observation in the study of hygrothermal aging on PBT-CSR[6] and SGF-CSR-PBT.[5] The low recovery of the toughness in all materials also indicates that the attack of absorbed water molecules on the PBT matrix was chemical in nature and caused permanent damage to the materials. Evidence of water molecule attack can be seen in the form of microcracks and micropores in the RD specimens of PBT, PBT/AX8900, and PBT/EXL2314 as shown in SEM micrographs (Figs. 2, 14, and 15). The tiny pores on the fracture surface are indications of the left over water molecules upon its removal. The micrographs also further explained the discrepancy of M_m values between the theory and the experiment, which was discussed earlier.

Flexural properties

Figure 16 shows the effect of immersion temperature on the flexural strength of various grades of PBT in the hygrothermal aging state. The flexural strength of all materials exhibited a similar reduction trend as in K_c and G_c as the immersion temperature increased. A higher reduction is observed when the immersion temperature is increased from 60 to 90°C. This can be attributed to intense hydrolysis that occurred above the T_g of PBT. However, such a dramatic reduction was not observed in SGF reinforced grades, i.e., PBT/

TABLE III
Effect of Immersion Temperature (30 and 90°C) on K_c and G_c Values of All Materials and the Extent of Deterioration

	AR		30°C				90°C			
			K_c ($MPam^{1/2}$)		G_c (kJ/m^2)		K_c ($MPam^{1/2}$)		G_c (kJ/m^2)	
	K_c ($MPam^{1/2}$)	G_c (kJ/m^2)	HA	RD	HA	RD	HA	RD	HA	RD
PBT	2.7	2.5	1.4	1.5 (54.9)	1.6	1.8 (7.09)	0.2	0.2 (9.0)	0.1	0.1 (5.7)
PBT/AX8900	4.7	9.0	2.7	2.1 (45.1)	8.1	4.2 (46.1)	0.3	0.4 (8.1)	0.1	0.2 (2.5)
PBT/EXL2314	4.0	6.2	3.5	3.0 (75.8)	11.4	8.0 (129.1)	0.3	0.3 (6.6)	0.1	0.2 (3.5)
PBT/SGF	3.4	4.8	3.1	3.4 (100.6)	3.5	5.6 (115.4)	2.2	2.4 (71.9)	2.0	2.6 (54.8)
PBT/AX8900/SGF	3.4	6.5	3.1	2.6 (76.5)	6.1	5.1 (78.7)	2.2	2.1 (60.3)	2.9	2.4 (36.9)
PBT/EXL2314/SGF	3.1	3.8	3.0	2.5 (80.1)	4.0	3.1 (81.5)	2.2	2.4 (78.4)	2.3	2.9 (75.3)

Values in parentheses are the % recoveries.

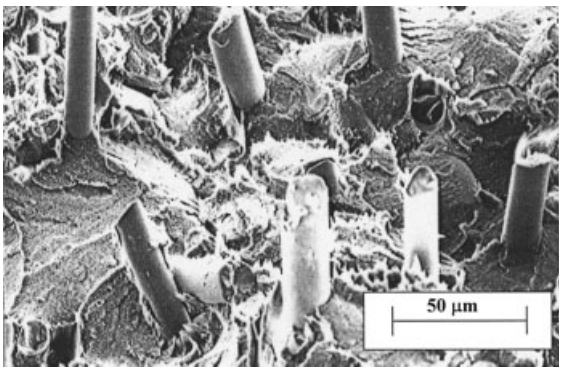

Figure 11 SEM micrograph of RD PBT/SGF after HA at 90°C.

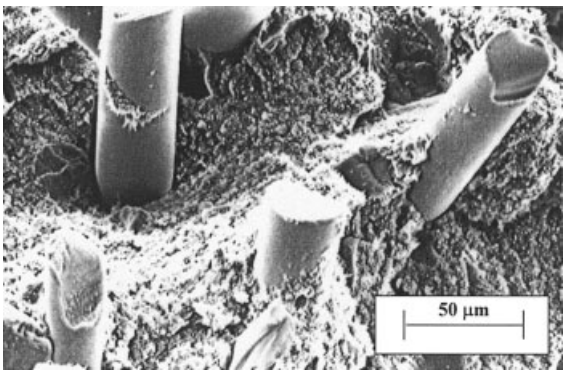

Figure 13 SEM micrograph of HA (90°C) specimen of PBT/EXL2314/SGF.

SGF, PBT/AX8900/SGF, and PBT/EXL2314/SGF. The complex orientation of the SGF provided micromechanical restriction to diffusion of the water molecules and subsequently reduced the hydrolysis of the PBT matrix. It is, therefore, indicated that SGF-RT-PBTs have better resistance to hygrothermal aging than RT-PBTs.

Figure 17 shows the effect of immersion temperature on the flexural modulus of all the materials. It was found that the flexural modulus was not much affected by the increase of temperature even up to 90°C. The maximum drop was only 24.3%, which was observed in PBT/EXL2314/SGF when the immersion temperature increased from 30 to 90°C. This observation can be attributed to the effect of heat on the rubber particles. The rubber particles degraded and became hard after exposure to high temperature, i.e., 90°C for ~ 450 h. The hardened rubber particles acted as rigid fillers in the system and, therefore, the modulus of the system did not deteriorate after hygrothermal aging. This is in agreement with the observations for K_c and G_c values. A reduction of fracture toughness is observed as the rubber particles lost their toughening effect after hygrothermal aging.

Table IV shows the flexural properties of various grades of PBT in AR, hygrothermal aging, and redried states. The result shows that both flexural strength and flexural modulus of specimens hygrothermally aged at 30°C were almost fully recovered upon redrying. This shows that the interaction of the water molecules and the matrix was merely physical. This situation at 90°C was quite different, as flexural strength was not fully recovered. This observation was more apparent in the case of PBT and unreinforced RT-PBT whereby % recoveries of 25–30% were recorded. However, higher % recoveries were reported in PBT/SGF (87.0%), PBT/AX8900/SGF (124.3%), and PBT/EXL2314/SGF (96.8%). This is in agreement with the results obtained in the fracture properties. The studies of hygrothermal aging of PBT-CSR and PBT-CSR-SGF by Mohd Ishak et al.[5,6] also reported similar observations. The increase in the flexural modulus in the redried specimen after hygrothermal aging at 90°C is noteworthy. The increase of the flexural modulus was due to the lost of plastication effect of the absorbed water molecules upon redrying. Another explanation for this observation is the hardening of the rubber particles due to long exposure to the hot environment as elaborated in the preceding para-

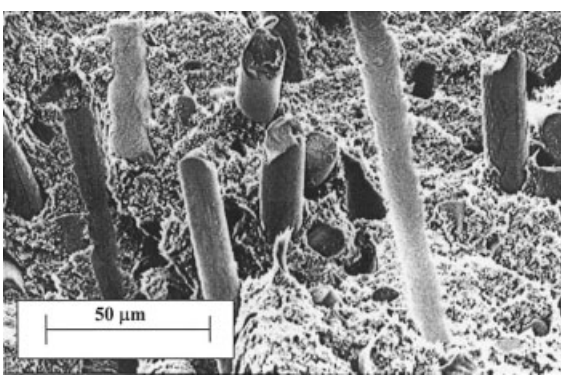

Figure 12 SEM micrograph of HA (90°C) specimen of PBT/AX8900/SGF.

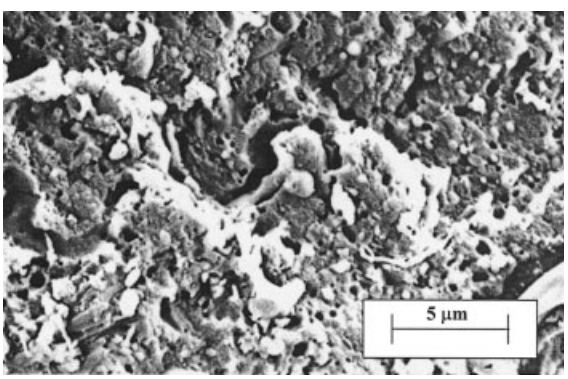

Figure 14 SEM micrograph of RD (90°C) specimen of PBT/AX8900.

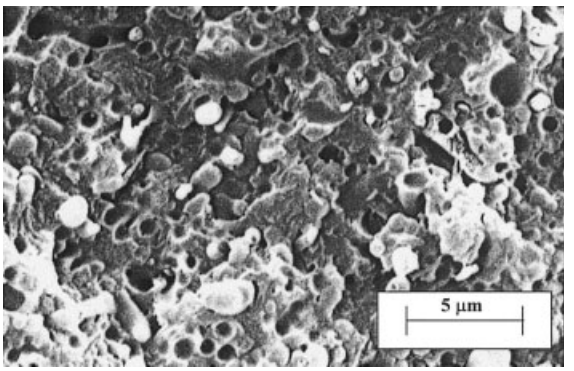

Figure 15 SEM micrograph of RD (90°C) specimen of PBT.

graph. This also explains the PBT without rubber toughening showed a much significant reduction in the modulus property, where it recorded a 16% drop compared to 6.31 and 4.37% for PBT/AX8900 and PBT/EXL2314, respectively, when the immersion temperature increased from 30 to 90°C as seen in Figure 17 and which could be calculated from the hygrothermal aging data in Table IV. Besides the hardening effect of rubbers, it was found that the hygrothermal aging resistance of SGF-reinforced grades of PBT and RT-PBT was relatively better than that of unreinforced grades. It can be seen from the % recoveries that the SGF-reinforced grades of materials generally are higher than those of unreinforced SGF materials (Table IV). However, between PBT/AX8900/SGF and PBT/EXL2314/SGF, the former exhibited a better resistance to hygrothermal aging and recovery upon redrying. This can be attributed to the lower hygroscopic acrylate content in AX8900 compared to EXL2314, which is a 100% acrylate product. Therefore, the hydrolysis damage caused by the attack of absorbed water is lesser in AX8900-toughened grades.

CONCLUSION

All materials, i.e., PBT, RT-PBTs, and SGF-RT-PBTs showed Fickian moisture absorption behavior and a strong dependency on the rubber types and presence of SGF as well as the immersion temperature. However, the diffusion rate of SGF-RT-PBTs was found to be lower than that of RT-PBTs and PBT. The hygrothermal aging at temperatures as low as 30°C has resulted in the decrease of K_c and G_c values for all materials. Furthermore, it was found that the deterioration caused by the water attack is irreversible by redrying the specimens. The deterioration caused by the hygrothermal aging was found to be more apparent in PBT and RT-PBTs while SGF-RT-PBTs showed a higher resistance to the hygrothermal aging. As to the water absorption behavior, EXL2314-toughened PBT exhibited more severe deterioration than AX8900-toughened PBT. A similar trend was observed in flex-

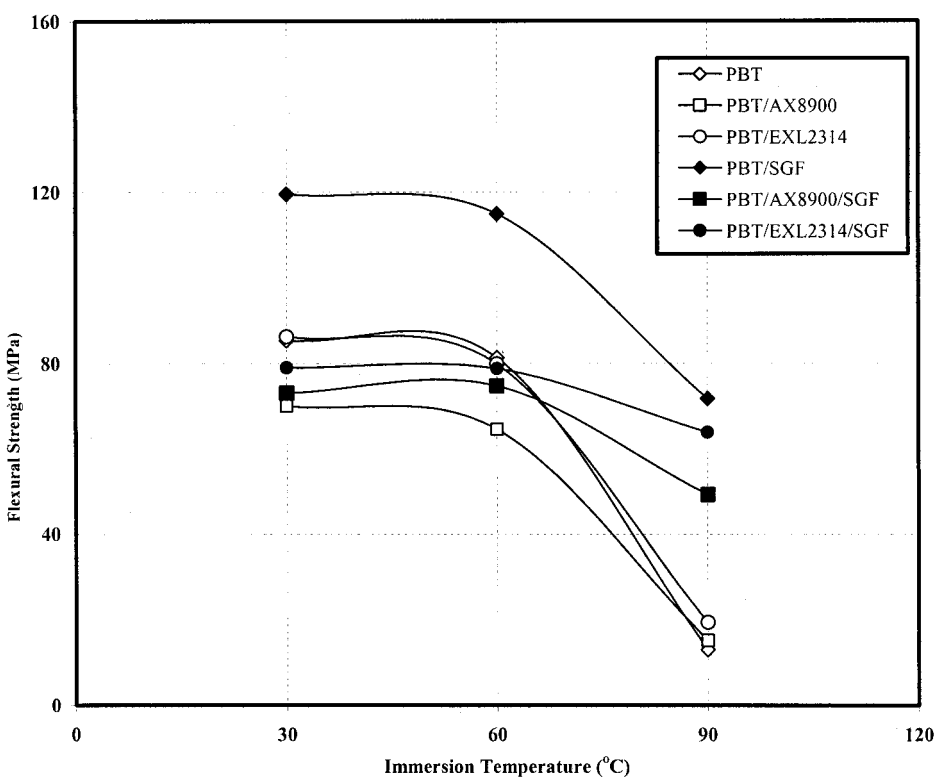

Figure 16 Effect of immersion temperature on flexural strength of various grades of PBT in HA state.

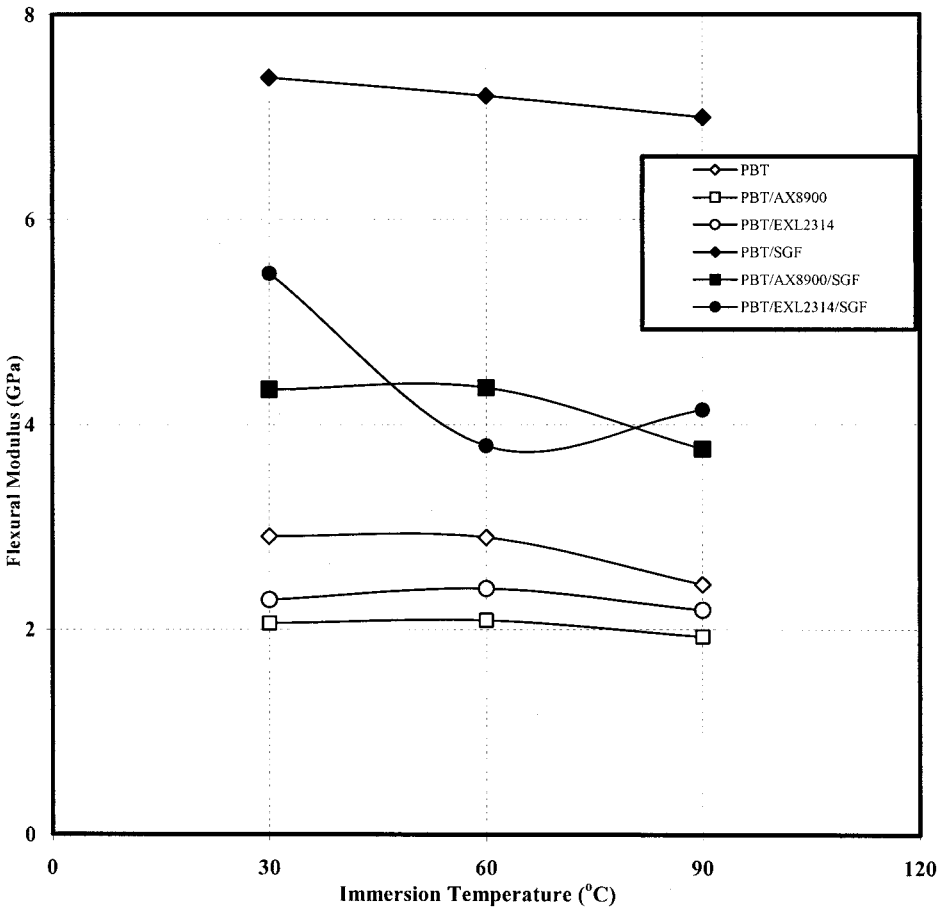

Figure 17 Effect of immersion temperature on flexural modulus of various grades of PBT in HA state.

ural strength, where a drastic decrease of the property was observed at immersion temperatures higher than 60°C. However, the flexural modulus of the materials did not deteriorate much by the immersion temperature. Again, the SGF-RT-PBTs were found to have relatively higher retention of the flexural properties against hygrothermal aging than that of RT-PBTs and PBT itself. Furthermore, between AX8900 and EXL2314, the former exhibited better resistance to hygrothermal aging and recovery upon redrying regardless of whether the system was reinforced by SGF. SEM micrographs revealed that the ability of PBT matrix to undergo plastic deformation and shear yielding was suppressed as a result of hygrothermal aging. In addition, permanent damage due to hydrolysis of PBT matrix was manifested by the microvoids observed on the fracture surface captured by SEM micrographs.

TABLE IV
Effect of Immersion Temperature (30 and 90°C) on Flexural Properties of All Materials and the Extent of Deterioration

	AR		30°C				90°C			
	Flexural strength (MPa)	Flexural modulus (GPa)	Flexural strength (MPa)		Flexural modulus (GPa)		Flexural strength (MPa)		Flexural modulus (GPa)	
			HA	RD	HA	RD	HA	RD	HA	RD
PBT	86.77	2.67	85.34	89.72 (103.4)	2.91	2.94 (110.1)	12.99	26.21 (30.2)	2.43	3.12 (116.8)
PBT/AX8900	66.33	1.96	70.11	58.24 (87.8)	2.06	2.16 (110.2)	15.14	17.09 (25.8)	1.93	2.22 (113.3)
PBT/EXL2314	79.91	2.31	86.23	86.22 (107.9)	2.29	2.49 (107.8)	19.37	21.99 (27.5)	2.19	2.59 (112.1)
PBT/SGF	112.95	6.07	119.53	125.38 (111.0)	7.38	7.40 (121.9)	71.71	98.25 (87.0)	6.99	7.66 (126.2)
PBT/AX8900/SGF	58.49	3.21	73.06	79.02 (135.1)	4.34	4.08 (127.1)	49.18	72.73 (124.3)	3.76	4.35 (135.5)
PBT/EXL2314/SGF	78.85	4.71	79.02	93.22 (118.2)	5.47	5.87 (124.6)	63.88	76.32 (96.8)	4.14	5.62 (119.3)

Values in parentheses are the % recoveries.

The authors present their appreciation to Universiti Sains Malaysia for the financial support on this project. We are also thankful to Professor J. Karger-Kocsis, from IVW, Kaiserslautern, Germany, Dr. C. A. Cruz Jr., from Rohm and Haas Company, USA, and Mr. Ved Sahajpal from Kureha Chemical, Singapore, for supplying the impact modifiers used in this study. The assistance of Mr. Ryuji Kobayashi from PPG, Japan, in providing the short glass fiber for the study is greatly appreciated.

References

1. Bucknall, C. B., Toughened Plastics; London: Applied Science, 1977.
2. Yow, B. N.; Ishiaku, U. S.; Mohd Ishak, Z. A.; Karger-Kocsis, J. J Appl Polym Sci 2002, 84, 1233–1244.
3. Boenig, H. V. Unsaturated Polyester: Structure and Properties; Elsevier: Amsterdam, 1964.
4. Golovoy, A.; Cheng M. F.; Van Oene, H. Polym Eng Sci 1988, 28, 200–206.
5. Mohd Ishak, Z. A.; Ishiaku, U. S.; Karger-Kocsis, J. Comp Sci Technol 2000, 60, 1–13.
6. Mohd Ishak, Z. A.; Ishiaku, U. S.; Karger-Kocsis, J. J Appl Polym Sci. 1999, 74, 2470–2481.
7. Williams, J. G. In Fracture Mechanics Testing Methods for Polymers and Adhesives and Composites, ESIS Publ. 28; Moore, D. R.; Pavan, A.; Williams, J. G., Eds.; Elsevier Science: Oxford, 2001; pp. 11–26.
8. Moore, D. R. In Fracture Mechanics Testing Methods for Polymers and Adhesives and Composites, ESIS Publ. 28; Moore, D. R.; Pavan, A.; Williams, J. G., Eds.; Elsevier Science, Oxford, 2001; pp. 59–71.
9. Mohd Ishak, Z. A.; Lim, N. C. Polym Eng Sci 1994, 34, 1645.
10. Mohd Ishak, Z. A.; Berry, J. P. J Appl Polym Sci 1994, 51, 2145.
11. Mohd Ishak, Z. A.; Ishiaku, U. S.; Karger Kocsis, J. J. Mater Sci 1999, 33, 3377.
12. Adams, R. K.; Hoeschele, G. K. In Thermoplastic Elastomers: A Comprehensive Review; Legge, N. R.; Holden, G.; Schoeder, H. E., Eds.; Hanser Publishers: Munich, 1987; pp. 163–196.
13. Hull, D.; Clyne, T. W. An Introduction To Composite Materials; Cambridge University Press: London, 1996.
14. Valentin, P.; Paray, F.; Guetta, B. J Mater Sci 1981, 22, 46–56.
15. Nigel, C. W. Br Polym J 1976, 10, 36–40.